Contents lists available at SciVerse ScienceDirect

Biochimica et Biophysica Acta

journal homepage: www.elsevier.com/locate/bbadis

Dietary curcumin counteracts extracellular transthyretin deposition: Insights on the mechanism of amyloid inhibition

Nelson Ferreira [a], Sónia A.O. Santos [b], Maria Rosário M. Domingues [c], Maria João Saraiva [a,d], Maria Rosário Almeida [a,d,*]

[a] IBMC, Instituto de Biologia Molecular e Celular, Universidade do Porto, Rua do Campo Alegre, 823, 4150-180 Porto, Portugal
[b] CICECO and Department of Chemistry, University of Aveiro, 3810-193 Aveiro, Portugal
[c] Mass Spectrometry Center, QOPNA, Department of Chemistry, University of Aveiro, 3810-193 Aveiro, Portugal
[d] ICBAS, Instituto de Ciências Biomédicas Abel Salazar, Universidade do Porto, Rua Jorge Viterbo Ferreira 228, 4050-313 Porto, Portugal

ARTICLE INFO

ABSTRACT

The transthyretin amyloidoses (ATTR) are devastating diseases characterized by progressive neuropathy and/or cardiomyopathy for which novel therapeutic strategies are needed. We have recently shown that curcumin (diferuloylmethane), the major bioactive polyphenol of turmeric, strongly suppresses TTR fibril formation *in vitro*, either by stabilization of TTR tetramer or by generating nonfibrillar small intermediates that are innocuous to cultured neuronal cells.

In the present study, we aim to assess the effect of curcumin on TTR amyloidogenesis *in vivo*, using a well characterized mouse model for familial amyloidotic polyneuropathy (FAP). Mice were given 2% (w/w) dietary curcumin or control diet for a six week period. Curcumin supplementation resulted in micromolar steady-state levels in plasma as determined by LC/MS/MS. We show that curcumin binds selectively to the TTR thyroxine-binding sites of the tetramer over all the other plasma proteins.

The effect on plasma TTR stability was determined by isoelectric focusing (IEF) and curcumin was found to significantly increase TTR tetramer resistance to dissociation. Most importantly, immunohistochemistry (IHC) analysis of mice tissues demonstrated that curcumin reduced TTR load in as much as 70% and lowered cytotoxicity associated with TTR aggregation by decreasing activation of death receptor Fas/CD95, endoplasmic reticulum (ER) chaperone BiP and 3-nitrotyrosine in tissues. Taken together, our results highlight the potential use of curcumin as a lead molecule for the prevention and treatment of TTR amyloidosis.

© 2012 Elsevier B.V. All rights reserved.

1. Introduction

Amyloidosis constitute a large group of acquired or hereditary disorders caused by extracellular deposition of abnormal insoluble fibrils composed of misfolded proteins or fragments thereof, which can damage tissue architecture and function, thus causing disease [1,2]. Nearly 30 different unrelated proteins, which share high content of lamellar cross β-sheet structure, are reported to be capable of forming amyloid fibrils *in vivo*, though they are associated with clinically distinct conditions [1,2].

Human transthyretin (TTR), carrier of virtually all of the retinol binding protein (RBP) in blood and about 15% of total thyroxine (T$_4$) in plasma, is associated with different forms of amyloidosis. That is the case of senile systemic amyloidosis (SSA), a late onset disease in which non-mutated TTR forms amyloid that deposits preferentially in the heart, affecting about 25% of individuals over 80 years, and the case of familial amyloidotic polyneuropathies (FAP) and cardiomyopathies (FAC) in which single amino acid substitutions resulting from single point mutations in the TTR gene result in deposition of amyloid aggregates in peripheral and autonomic nervous systems and heart, respectively [3,4].

Regarding hereditary TTR-related amyloidosis, since the first report describing the TTR V30M mutant, the most common among FAP patients [5], more than one hundred TTR variants have been found to cause TTR amyloidosis (amyloidosismutations.com). The amyloidogenic potential of the TTR variants has been related to the decrease of protein tetramer conformational stability [6], which leads to its dissociation into partially unfolded non-native monomeric species, the rate-limiting step for the process of amyloid fibril formation associated to neurodegeneration and cell death [7]. Moreover, studies using a combination of polyacrylamide gel electrophoresis (PAGE) and isoelectric focusing (IEF) under semi-dissociating conditions have shown that amyloidogenic TTR tetramers present a greater tendency to dissociate compared with wild-type (WT) TTR [8]. It has been shown that binding of T$_4$ to TTR efficiently inhibits TTR fibrillogenesis *in vitro* and does so by stabilizing the tetramer against dissociation, thus preventing the

* Corresponding author at: IBMC, Instituto de Biologia Molecular e Celular, Rua do Campo Alegre, 823, 4150-180 Porto, Portugal. Tel.: +351 226074900; fax: +351 226099157.
E-mail address: ralmeida@ibmc.up.pt (M.R. Almeida).

subsequent conformational alterations required for amyloid fibril formation [9]. Accordingly, it has been proposed that small aromatic molecules might act analogously by binding preferentially to the central hydrophobic channel and stabilizing the native state of TTR over its dissociative transition state [7]. Very recently, our group reported that curcumin (diferuloylmethane), a naturally occurring polyphenol, competes with T_4 for the binding to TTR and inhibits different steps of the process of TTR amyloid fibril formation *in vitro* [10]. In the current work, we present the *in vivo* effects of curcumin using a well characterized FAP mice model.

2. Materials and methods

2.1. Ethics statement

All the experiments described herein were approved by the Portuguese General Veterinarian Board (authorization number 024976 from DGV-Portugal) and are in compliance with national rules and the European Communities Council Directive (86/609/EEC), for the care and handling of laboratory animals.

2.2. Transgenic mice

Seven month-old transgenic mice for human TTR V30M in a TTR null background [11], labeled as hTTR V30M mice, were fed either standard mouse chow (controls, $n = 10$) or standard mouse chow containing 2% (w/w) curcumin (Sigma-Aldrich, St. Louis, MO, USA) (treated, $n = 10$) over 6 weeks. After the treatment period, animals were sacrificed following anesthesia with ketamine/xylazine and blood samples were collected. Plasma was separated by centrifugation and stored at -20 °C prior to analysis. Mice tissues, in particular whole gastrointestinal tract (GI), including esophagus, stomach, colon and duodenum, were immediately excised and frozen at -80 °C or fixed in 4% neutral buffered formalin and embedded in paraffin for light microscopy techniques.

2.3. Analytical procedure and sample preparation for the determination of curcumin in mice plasma

The frozen plasma samples were thawed at room temperature. Then, 0.3 ml of 134 U/ml β-glucuronidase solution in sodium acetate buffer (pH 5.0) was added to 100 μl of each plasma. The mixtures were vortexed and incubated at 37 °C for 1 h. The buffered plasmas were extracted with 2 ml of ethyl acetate by vortex mixing for 2 min. After centrifugation at 2000 rpm for 2 min, the upper organic layer was removed into a clean microcentrifuge tube and evaporated to dryness under nitrogen stream. The extracts were re-suspended in 200 μl of methanol.

2.3.1. Chromatographic procedure

The HPLC system consisted of a variable loop Accela autosampler, an Accela 600 LC pump and an Accela 80 Hz PDA detector (Thermo Fisher Scientific, San Jose, CA, USA). Analyses were carried out in using a Supelco Discovery® C-18 (15 cm × 2.1 mm × 5 μm) column (Agilent Technologies, Waldbronn, Germany). The compounds were separated using a gradient elution program at a flow rate of 0.2 ml min^{-1}, at 25 °C. The mobile phases consisted in water:acetonitrile (90:10, v/v) (A) and acetonitrile (B), both with 0.1% of formic acid. The following linear gradient was applied: 0–20 min: 0–100% B; 20–23 min: 100% B; 23–30 min: 100–0% B; followed by re-equilibration of the column for 10 minutes before the next run. Single online detection was carried out in DAD detector, at 280 nm, and UV spectra in a range of 210–600 nm were also recorded.

2.3.2. ESI–MS^n analysis

The HPLC system was coupled to a LCQ Fleet ion trap mass spectrometer (Thermo Finnigan, San Jose, CA, USA) with an ESI source

and operating in negative mode. The spray voltage was 5 kV and capillary temperature 300 °C. The capillary and tune lens voltages were set at -28 V and -115 V, respectively. CID-MS^n experiments were performed on mass-selected precursor ions in the range of m/z 100–1000. The scan time was equal to 100 ms and the collision energy was optimized between 15 and 40 (arbitrary units), using helium as collision gas. Data were acquired using Xcalibur® data system (Thermo Finnigan, San Jose, CA, USA).

2.3.3. Calibration curve

The curcumin calibration curve was obtained taking into account the possibility of a non-complete efficient extraction. Thus, six different concentrations of curcumin standards were added to plasma control samples in the range 0.7–14 μM. The samples were then extracted using the methodology above described. The injection in HPLC, under the same chromatographic conditions, gave a linear regression between the peak area and concentration (expressed as μg ml^{-1}) with $R^2 = 0.982$, intercept of 948224 and slope of 2.87×10^6. The detection range was established from 0.36 to 1.20 μg ml^{-1}.

2.4. Determination of TTR levels in mice plasma by sandwich enzyme-linked immunosorbent assay (ELISA)

The concentration of plasma TTR was determined by ELISA. Briefly, 96-well plates (Nunc, Roskilde, Denmark) were coated overnight at 4 °C, with rabbit anti-human TTR polyclonal antibody (Abcam, Cambridge, UK). After blocking and washes, TTR standards (2–25 ng/ml) and the diluted mice plasma were applied to different wells in triplicate and incubated. Following sheep anti-human TTR was added and incubated for one hour (Abcam, Cambridge, UK). After washing, anti-sheep conjugated alkaline phosphatase was added. p-Nitrophenyl phosphatase was employed in color development. The absorbance was measured at 405 nm in a Multiskan® Ascent microplate spectrophotometer (Thermo Electron Instruments). Data were fitted to 2nd-order polynomial (quadratic equation).

2.5. Thyroxine (T_4) binding gel electrophoresis

Five microliters of plasma from curcumin treated mice and from controls (non-treated mice) were incubated with [^{125}I]-T_4 (specific radioactivity 1250 μCi/μg; Perkin–Elmer, MA, USA). The plasma proteins were then separated by native PAGE [12]. The gel was dried, subjected to phosphor imaging (Typhoon 8600; Molecular Diagnostics, Amersham Biosciences), and analyzed using the ImageQuant program version 5.1.

2.6. Isoelectric focusing (IEF) in semi-dissociating conditions

Thirty microliters of mice plasma from treated and non-treated animals were subjected to native electrophoresis (PAGE). The TTR gel band was excised and applied to a semi-dissociating (4 M urea) pH 4–6.5 IEF gel run for 6 hours at 1200 V [12]. Proteins were stained with Coomassie Blue. The gels were scanned and subjected to densitometry analysis using the ImageQuant program version 5.1.

2.7. Immunohistochemistry

Tissue sections (5 mm thick) were deparaffinated in histoclear and dehydrated in a descent alcohol series. Endogenous peroxidase activity was inhibited with 3% hydrogen peroxide/ 100% methanol, and sections were blocked in 4% fetal bovine serum and 1% bovine serum albumin in PBS. The primary antibodies and the respective dilutions used were: rabbit polyclonal anti-TTR (1:1000) (Carpinteria, CA, USA), goat polyclonal anti-BiP (1:50) and rabbit polyclonal anti-Fas (1:200) (Santa Cruz Biotechnology, Santa Cruz, CA, USA), rabbit polyclonal anti-3-nitrotyrosine (1:500) (Chemicon, Temecula,

CA, USA), which were diluted in blocking solution and incubated overnight at 4 °C. Antigen visualization was performed with the biotin–extravidin peroxidase kit (Sigma-Aldrich, St. Louis, MO, USA) using hydrogen peroxide and diaminobenzidine as substrate and chromogen, respectively. Immunohistochemistry analysis was carried out independently by two investigators unaware of the origin of the tested tissue sections. Semi-quantitative immunohistochemical (SQ-IHC) analysis was performed using Image-Pro Plus version 5.1 software. This application enables the measurement of the area occupied by pixels corresponding to the immunohistochemical substrate's color that is normalized relatively to the total area. Each slide was analyzed in five different representative areas.

2.8. Total protein extracts and Western blot analysis

Mice tissues (approximately 5 mg), in particular stomach and colon, were homogenized on ice in a small glass rod homogenizer with 300 μl of lysis buffer containing 5 mM EDTA, 2 mM EGTA, 20 mM MOPS, 1% Triton X-100, 1 mM PMSF and Protease Inhibitor Mix (GE Healthcare). After centrifugation (14,000 rpm for 20 min at 4 °C) protein concentration in the supernatant was determined by the Bradford protein assay (Bio-Rad, CA, USA). Fifty micrograms of total protein from each tissue were separated on 15% SDS–PAGE and transferred onto a nitrocellulose Hybond-C membrane using a Mini Trans-Blot Cell (Bio-Rad) system. The primary antibodies and the respective dilutions used were: rabbit polyclonal anti-TTR (1:1000) (Carpinteria, CA, USA), rabbit polyclonal anti-BiP (1:1000) (Abcam, Cambridge, UK) and mouse polyclonal GAPDH (1:1000) (Santa Cruz Biotechnology, Santa Cruz, CA, USA). Detection was performed with ECL® (GE Healthcare, Buckinghamshire, UK). Quantification of blots was performed with a Bio-Rad ChemiDoc XRS system using the IMAGELAB software, and immunosignals were normalized with GAPDH expression. Results are presented as normalized density $\pm$ SD.

3. Results

3.1. Dietary curcumin administration results in stable levels in plasma

In the present study, we aimed to study the effect of subchronic supplementation of curcumin at an early stage of the pathogenesis, because previous in vitro studies demonstrated that curcumin inhibits TTR aggregation and TTR aggregates deposition and associated cytotoxicity begin prior to amyloid formation. We used the hTTR V30M mice that present deposition of non-fibrillar mutant TTR starting at approximately 6 months of age; TTR amyloid fibrils are typically detected after 1 year of age or later and the deposition occurs mainly at the gastrointestinal tract.

Mice were fed *ad libitum* a diet consisting of standard mouse chow with 2% (w/w) curcumin. This intermediary dosage was selected based upon available *in vivo* reports [13–15]. Quantification of TTR in mice plasma from untreated and curcumin treated hTTR V30M mice revealed no significant difference between the two groups (389 $\pm$ 172 μg TTR/ml and 441 $\pm$ 96 μg TTR/ml, respectively), indicating that curcumin treatment did not interfere with TTR plasma levels in vivo.

We measured curcumin plasma levels by LC/MS/MS analysis. Mice fed with curcumin diet reached a steady-state plasma concentration of 21.4 $\pm$ 3.6 μM total curcumin (unconjugated and metabolites) at the end of the treatment period. No curcumin was detected in untreated mice plasma. As expected from previous studies using similar or higher doses *in vivo*, dietary supplementation of curcumin was well tolerated and non-toxic [14,16]. Weight gain in the control and curcumin-fed group was identical over the 6-weeks period of treatment (results not shown). No liver toxicity was detected by histological evaluation of hematoxylin and eosin stained liver sections.

3.2. Curcumin selectively binds to TTR in plasma

The interaction of curcumin with TTR *in vivo* was confirmed by analysis of plasma, from treated and control mice, after incubation with radiolabelled T_4 ($[^{125}I]$-T_4) and separation of plasma T_4-binding proteins by gel electrophoresis in native conditions and visualization after autoradiography of the dried gel as can be seen in Fig. 1A. Phosphor imaging analysis of the gels (Fig. 1A) showed that, in control mice, three main proteins bound T_4: the main binding protein was TTR (62.48% $\pm$ 12.46 of total T_4) followed by albumin (26.96% $\pm$ 6.52) and TBG (T_4 binding globulin, 10.56% $\pm$ 7.41). The results showed less $[^{125}I]$-T_4 binding to plasma TTR (36.19% $\pm$ 12.21) from curcumin treated mice, indicating that curcumin mediated a potent inhibition (42% decrease) of binding of T_4 to TTR. Displacement of $[^{125}I]$-T_4 from plasma TTR by curcumin resulted in more intense TBG bands due to the higher binding affinity of T_4 to TBG than to albumin.

3.3. Curcumin treatment increases plasma TTR resistance to dissociation

The effect of curcumin on plasma TTR tetramer stabilization was investigated by IEF in the presence of 4 M urea. Plasma samples from treated hTTR V30M and control mice were compared concerning band patterns and tetramer/total protein ratios. Under the tested conditions, plasma TTR presented a characteristic band pattern composed of monomer, an oxidized monomer and several lower pI bands corresponding to different forms of tetramers (Fig. 1B). The results showed that mice treated with curcumin presented a significant increase of TTR stability as evidenced by the higher tetramer/total protein ratio (0.45) when compared to control animals (0.29) (Fig. 1B).

3.4. Curcumin decreases non-fibrillar TTR deposition and associated biomarkers

The effect of curcumin on non-fibrillar TTR deposition in different tissues was investigated by semi-quantitative immunohistochemical analysis (SQ-IHC) and Western blotting. At the end of treatment, mice were 8.5 month-old and, as expected at this age, control mice displayed widespread TTR staining along the gastrointestinal (GI) tract. In contrast, curcumin treated mice exhibited significant reduction of TTR load in all GI tract organs analyzed. In stomach, the main organ of TTR deposition in hTTR V30M mice, we detected a decrease of approximately 58% of TTR aggregates as can be seen in the representative IHC images and respective quantification (Fig. 2A). These results were further confirmed by Western blot analysis of TTR levels after normalization to GAPDH signal intensities.

Moreover, the highest reduction in TTR staining was obtained in the intestine, particularly in colon (86% decrease) (Fig. 3A). We next searched for activation of several tissue markers previously associated with TTR extracellular deposition [17–19], including ER-resident chaperone BiP, Fas receptor (CD95) and 3-nitrotyrosine.

By semi-quantitative IHC, we found a decrease of approximately 75% of the ER chaperone BiP in the stomach of curcumin treated mice, as compared to the untreated control group (Fig. 2A). Results were confirmed by Western blot of stomach lysates (Fig. 2B). Likewise, a significant decrease of BiP immunoreactivity was found in colon (63% decrease) as can be seen in Fig. 3A. BiP quantification by Western blot analysis colon of lysates corroborated the IHC results (Fig. 3B).

We also investigated the engagement of death receptors on the cell surface typically up-regulated in tissues from patients affected with TTR-associated amyloidoses, in particular Fas receptor (CD95). Immunostaining analysis of mice tissues showed that treated mice presented reduced levels of Fas in the stomach and colon (Figs. 2A and 3A, respectively).
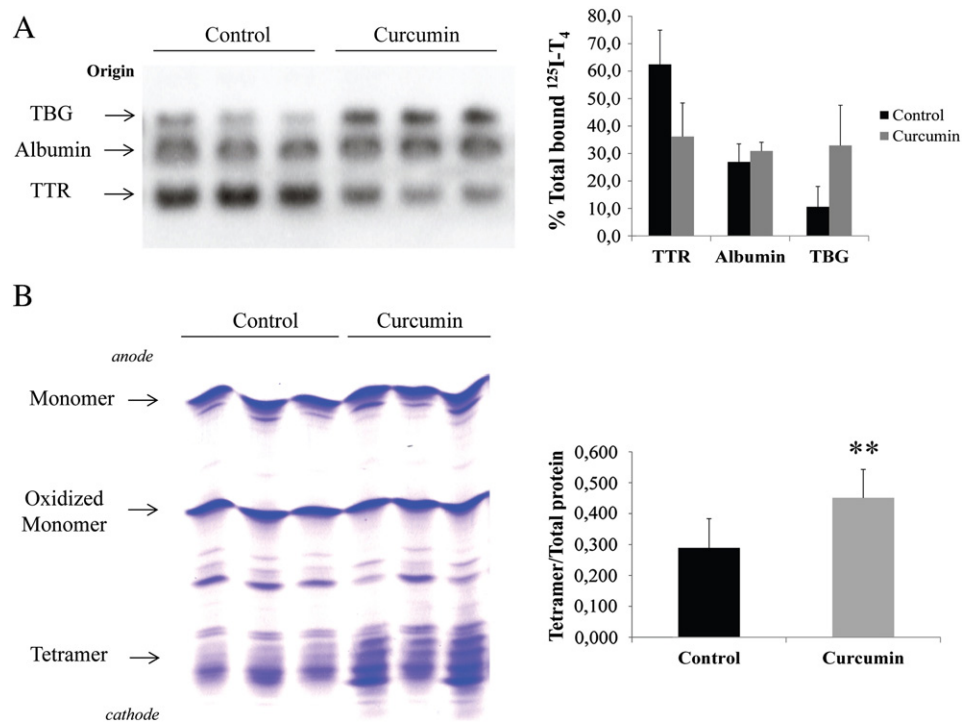
Fig. 1. Curcumin binds to TTR in plasma and increases TTR resistance to dissociation. (A) Representative PAGE analysis of [125I]-T4 distribution among T4 binding proteins after incubation with plasma from treated and non-treated hTTR V30M mice. Different plasma T4 binding proteins are indicated. The histogram shows percentage of total bound [125I]-T4 to each plasma T4 binding protein. (B) Plasmas from mice treated with curcumin and controls were subjected to isoelectric focusing analysis (IEF) under semi-dissociating conditions. Different TTR molecular species are indicated. The histogram shows TTR tetramer/total TTR bands ratio obtained after densitometry analysis of IEF gels for both treated and untreated groups of 10 animals each ([**]$P < 0.01$).

Nitration of tyrosine residues of proteins has been suggested as a marker of peroxynitrite-mediated tissue injury in TTR amyloidosis [17]. Thus, we next searched for activation of the 3-nitrotyrosine (3-NT) by IHC and found a decrease of 64% and 78%, respectively, in the stomach and colon of curcumin treated mice, as compared to the untreated control group (Figs. 2A and 3A, respectively).

4. Discussion

There are multiple lines of compelling evidence indicating that curcumin, the main biologically active phytochemical of *Curcuma longa*, can be useful for the prevention and treatment of several types of neurodegenerative diseases.

Curcumin is capable of dose-dependently inhibit Aβ aggregation and disaggregate pre-formed Aβ fibrils [20] and this seems to depend on fibril-related conformational structure rather than primary sequence [21]. In addition, curcumin blocks Aβ42 oligomer toxicity and increases cell viability in SH-SY5 human neuroblastoma cells [21]. When fed to transgenic mouse models of Alzheimer's disease curcumin has been shown to cross the blood–brain barrier (BBB), label plaques and reduce amyloid levels and plaque burden, resulting in reduced cognitive deficits and neuroinflammation [21,22]. Beyond AD, oral curcumin efficacy has been recently shown in a knock-in mouse model of Huntington's disease, receiving a curcumin diet since conception until 4.5 months of age. At the end of the treatment, mice presented decreased huntingtin aggregates, improvement of neuropathology and transcriptional deficits and partial behavioral improvement [23].

With regard to TTR amyloidosis, we and other authors reported that curcumin binds to WT and mutant TTR and increases its conformational stability both *in vitro* and *ex vivo* [10,24]. We have also characterized the effects of curcumin on TTR aggregation *in vitro* [10]. We demonstrated that curcumin induces TTR oligomerization into a homogeneous population of small spherical aggregates as assayed by transmission electron microscopy (TEM) and dynamic light scattering

(DLS). When incubated with Schwannoma cells, curcumin-generated oligomers were shown to decrease caspase-3 activation as compared with "on-pathway" intermediates, thus indicating that curcumin redirects TTR aggregation cascade. Moreover, curcumin was also found to act as amyloid fibril disruptor *in vitro*.

Herein, we investigated the *in vivo* effects of curcumin on TTR deposition in a FAP mice model by subchronic oral supplementation with curcumin. A wide range of doses (0.05%–5% w/w in chow) have been used to test curcumin efficacy in different mouse models of aging, neuroinflammation and tumorigenesis [25]. We chose a dosage (2%) that has been proven to be safe and is well within the range of those formerly reported to produce steady-state levels of curcumin in plasma and gastrointestinal mucosa *in vivo* [16,26].

In the present study, mice fed with curcumin reached a relatively high plateau concentration of $21.4 \pm 3.6\ \mu M$ in plasma that resulted in a potent competition with T4 (42%) for the binding to TTR. In addition, selective binding of curcumin to the largely unoccupied T4 binding sites significantly inhibited tetramer dissociation into non-native monomeric intermediaries under semi-dissociating conditions. This observation is consistent with one of the most likely therapeutic approaches for the disease, by which small molecule interactions at the weaker dimer–dimer interface might stabilize the native state of TTR over the dissociative transition state, thus preventing amyloidogenesis cascade from beginning [7]. Indeed, we further demonstrate that curcumin chronic administration significantly lowers TTR load in tissues, particularly along the gastrointestinal tract.

In FAP, intertwined activation of pathways leading to apoptosis, ER-mediated stress response and oxidative damage have been observed in tissues presenting extracellular TTR deposition but not specialized in TTR synthesis [27]. Our results indicate significant decrease of Fas-death receptor, ER-resident chaperone BiP and 3-nitrotyrosine levels in the vicinity of the deposits, which is in accordance with curcumin inhibitory effect on TTR aggregation and suggestive of reduction of cytotoxicity and phenotype recovery/tissue improvement.
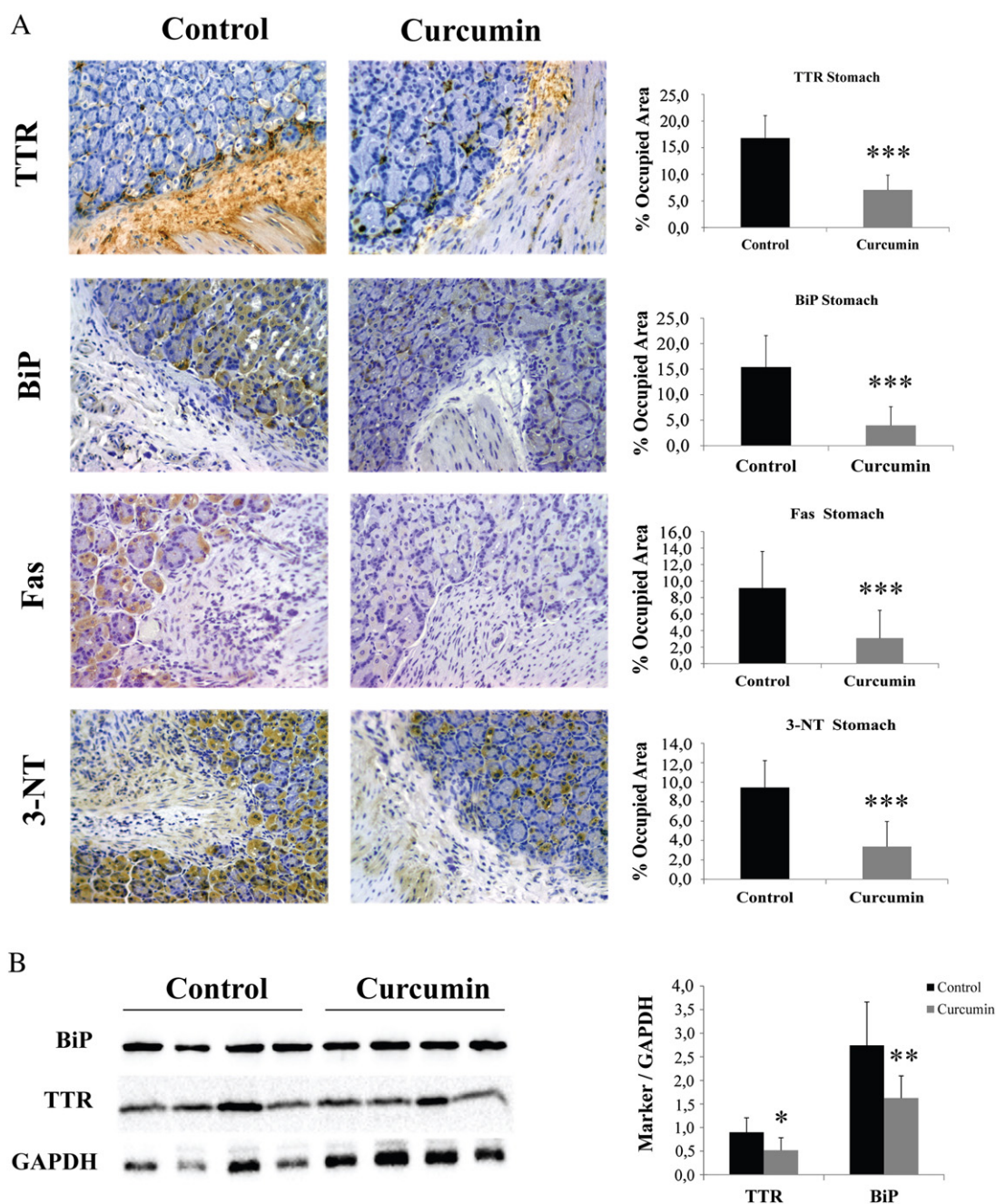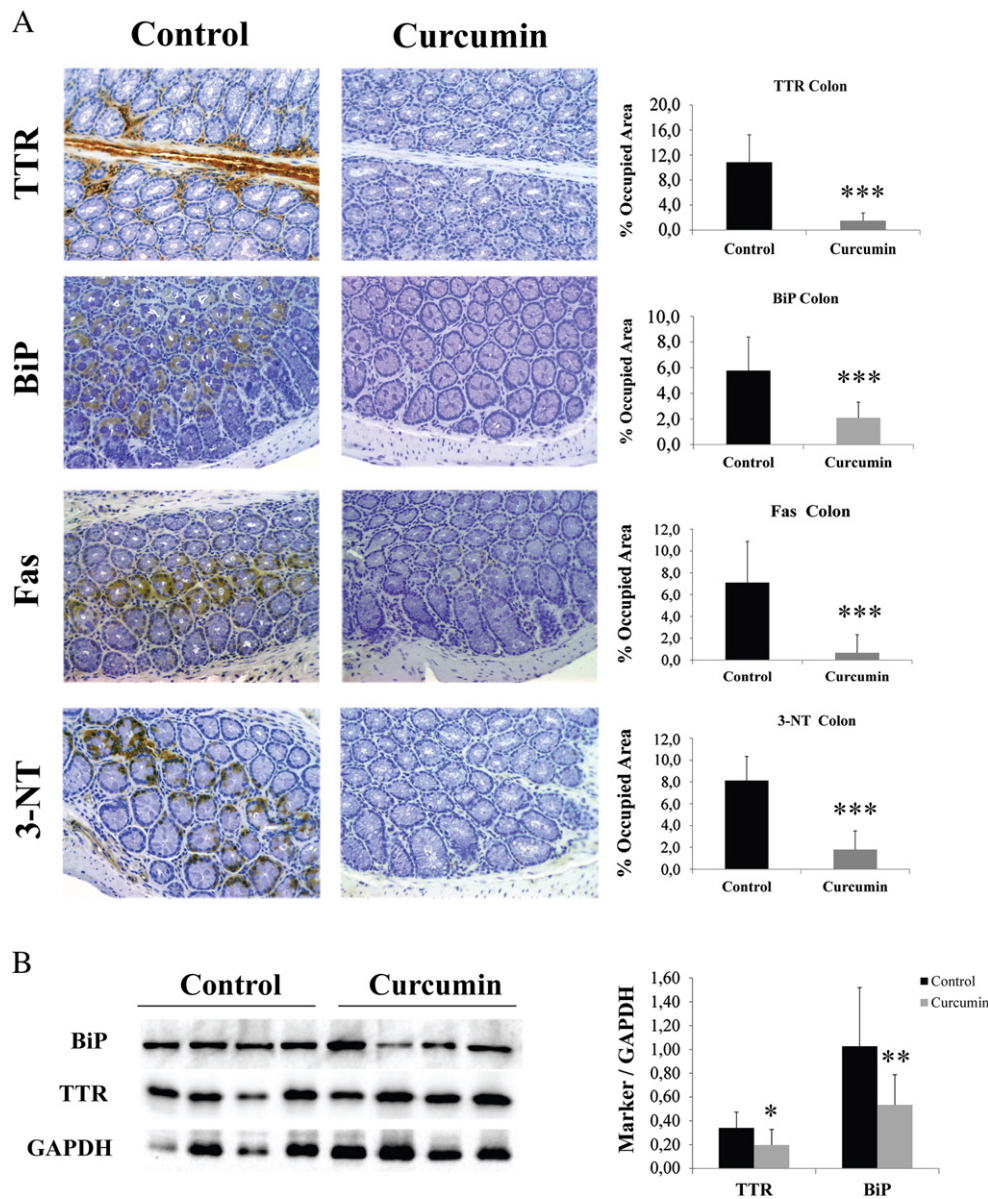
Fig. 2. Curcumin supplementation decreases TTR deposition and associated biomarkers in stomach of hTTR V30M mice. (A) Representative immunohistochemistry analysis of TTR, BiP, Fas and 3-nitrotyrosine in colon of hTTR V30M mice fed with curcumin (right panels) and age-matched controls (left panels); 20× magnification. Histogram: quantification of immunohistochemical images is represented as percentage of occupied area ± SD ($^{***}P<0.005$). (B) Representative anti-BiP and anti-TTR Western blots of stomachs from TTR V30M mice treated with curcumin and non-treated mice. Histogram: normalized BiP/GAPDH and TTR/GAPDH density quantifications ± SD ($^{*}P<0.05$; $^{**}P<0.01$).

Though our data clearly indicate that curcumin mediates its effects by directly modulating the TTR misfolding cascade, we speculate that other important pharmacological aspects of curcumin may actually potentiate its anti-amyloidogenic/neuroprotective effects *in vivo*. It is widely accepted that inflammation and oxidative impairment play a key role in the process of amyloid deposition, and therapies that specifically block oxidative-inflammatory signaling pathways may mitigate amyloid pathology [28,29]. Actually, curcumin treatment has been proven effective in inhibiting several mediators of inflammation, including interleukin (IL)-1β, phospho-c-Jun NH2-terminal kinase (pJNK), nitrotyrosine and inducible nitric-oxide synthase (iNOS) while reducing Aβ plaque deposition in AD models [30,31]. Furthermore, it has been reported that natural curcuminoids restore Aβ phagocytosis by AD peripheral blood

mononuclear cells (PBMCs), thus suggesting an immune-mediated approach to stimulate uptake and clearance of Aβ peptide by AD patients innate immune cells [32,33].

Over the past decades, different non-invasive therapeutic measures have been suggested against TTR amyloidosis. Small molecules presenting structural complementarity to the T_4 binding sites within TTR, including non-steroidal anti-inflammatory drugs (NSAIDs) such as flufenamic acid and diflunisal, and its derivatives, have been proposed for FAP treatment by acting as TTR kinetic stabilizers [12,34]. Recently, tafamidis meglumine, a potent inhibitor of TTR dissociation, (Fx-1006A) has completed Phase II/III trials for the treatment of FAP [35].

Given the clinical and genetic heterogeneity of TTR amyloidosis, it has become increasingly clear that combination therapies may improve

Fig. 3. Curcumin supplementation decreases TTR deposition and associated biomarkers in colon of hTTR V30M mice. (A) Representative immunohistochemistry analysis of TTR, BiP, Fas and 3-nitrotyrosine in stomach of hTTR V30M mice fed with curcumin (right panels) and age-matched controls (left panels); 20× magnification. Histogram: quantification of immunohistochemical images is represented as percentage of occupied area ± SD ($^{***}P<0.005$). (B) Representative anti-BiP and anti-TTR Western blots of colon from hTTR V30M mice treated with curcumin and non-treated mice. Histogram: normalized BiP/GAPDH and TTR/GAPDH density quantifications ± SD ($^{*}P<0.05$; $^{**}P<0.01$).

treatment efficacy and clinical outcome by acting synergistically to reduce TTR amyloidogenicity. Recently, our laboratory has reported that epigallocatechin-3-gallate (EGCG), the main polyphenol constituent of green tea, inhibits TTR fibrillogenesis by a different mode of interaction that does not encompass the hydrophobic T_4 binding pockets [36,37]. The crystal structure of the TTR-EGCG complex indicated three novel binding sites for EGCG on TTR, all located at the molecule surface. The structural data suggested a more rigid binding of EGCG to the binding site located in a region of the TTR tetramer that allows contact of EGCG with both TTR dimers, thereby stabilizing the TTR tetramer [38]. The other two binding sites are found at different monomers in the TTR molecule and may be involved in the oligomerization of TTR tetramers, resulting in the formation of small "off-pathway" aggregates [36,38] that are innocuous to neuronal cells [10,38]. Moreover, Kristen and colleagues further supported these observations by showing an inhibitory effect of green tea and/or green tea extract on the progression of cardiac TTR amyloidosis [39].

Since both curcumin and EGCG are able to redirect TTR misfolding and cytotoxicity, although by different molecular mechanisms of action, it seems plausible to speculate whether a combined treatment using both compounds might synergistically increase their clinical beneficial effects on TTR pathology.

While curcumin appears to be non-toxic and well-tolerated in humans, even in clinical trials for the treatment of inflammatory bowel disease and colorectal cancer [25], some concerns regarding its poor oral bioavailability have been raised [40].

The average curcumin peak serum concentration achieved in a Phase I clinical trial, where 4–8 g/day of curcumin were orally administrated for 3 months, was 0.41–1.75 μM (lower than that obtained in our study) [41]. In order to increase those levels and the biological activity of curcumin, several strategies have been proposed. Some are directed towards the development of curcumin structural analogs, and others to different routes of administration or delivery systems, namely by the use of nanoparticles or liposomes. The use of adjuvants

modulating curcumin metabolic and elimination pathways has also been tested. That is the case of piperine, a known inhibitor of hepatic and intestinal glucuronidation, which when administered concomitantly with curcumin results in 2000% increase bioavailability in humans [41]. Even though, more and longer studies are necessary to confirm the effectiveness of such strategies. Currently, the efficacy of curcumin on Alzheimer's disease (AD) progression is being tested by clinical trials for Mild Cognitive Impairment (MCI) or mild Alzheimer's Disease (clinicaltrials.gov) using doses up to 6 g/day.

In conclusion, the present study demonstrated that dietary curcumin modulates TTR amyloidogenicity *in vivo*, and points towards the potential use of curcumin as a lead molecule for the design of new TTR amyloid inhibitors.

Acknowledgments

References

[1] P. Westermark, Aspects on human amyloid forms and their fibril polypeptides, FEBS J. (2005) 5942–5949.

[2] M.B. Pepys, Amyloidosis, Annu. Rev. Med. 57 (2006) 223–241.

[3] Y. Ando, M. Nakamura, S. Araki, Transthyretin-related familial amyloidotic polyneuropathy, Arch. Neurol. 62 (2005) 1057–1062.

[4] C. Rapezzi, C.C. Quarta, L. Riva, S. Longhi, I. Gallelli, M. Lorenzini, P. Ciliberti, E. Biagini, F. Salvi, A. Branzi, Transthyretin-related amyloidoses and the heart: a clinical overview, Nat. Rev. Cardiol. 7 (2010) 398–408.

[5] M.J. Saraiva, S. Birken, P.P. Costa, D.S. Goodman, Amyloid fibril protein in familial amyloidotic polyneuropathy, Portuguese type. Definition of molecular abnormality in transthyretin (prealbumin), J. Clin. Invest. 74 (1984) 104–119.

[6] A. Quintas, M.J. Saraiva, R.M. Brito, The amyloidogenic potential of transthyretin variants correlates with their tendency to aggregate in solution, FEBS Lett. 418 (1997) 297–300.

[7] S.M. Johnson, R.L. Wiseman, Y. Sekijima, N.S. Green, S.L. Adamski-Werner, J.W. Kelly, Native state kinetic stabilization as a strategy to ameliorate protein misfolding diseases: a focus on the transthyretin amyloidosis, Acc. Chem. Res. 38 (2005) 911–921.

[8] K. Altland, P. Winter, Potential treatment of transthyretin-type amyloidoses by sulfite, Neurogenetics 2 (1999) 183–188.

[9] G.J. Miroy, Z. Lai, H.A. Lashuel, S.A. Peterson, C. Strang, J.W. Kelly, Inhibiting transthyretin amyloid fibril formation via protein stabilization, Proc. Natl. Acad. Sci. U. S. A. 93 (1996) 15051–15056.

[10] N. Ferreira, M.J. Saraiva, M.R. Almeida, Natural polyphenols inhibit different steps of the process of transthyretin (TTR) amyloid fibril formation, FEBS Lett. 585 (2011) 2424–2430.

[11] K. Kohno, J.A. Palha, K. Miyakawa, M.J. Saraiva, S. Ito, T. Mabuchi, W.S. Blaner, H. Iijima, S. Tsukahara, V. Episkopou, M.E. Gottesman, K. Shimada, K. Takahashi, K. Yamamura, S. Maeda, Analysis of amyloid deposition in a transgenic mouse model of homozygous familial amyloidotic polyneuropathy, Am. J. Pathol. 150 (1997) 1497–1508.

[12] M.R. Almeida, B. Macedo, I. Cardoso, I. Alves, G. Valencia, G. Arsequell, A. Planas, M.J. Saraiva, Selective binding to transthyretin and tetramer stabilization in serum from patients with familial amyloidotic polyneuropathy by an iodinated diflunisal derivative, Biochem. J. 381 (2004) 351–356.

[13] S.V. Singh, X. Hu, S.K. Srivastava, M. Singh, H. Xia, J.L. Orchard, H.A. Zaren, Mechanism of inhibition of benzo[a]pyrene-induced forestomach cancer in mice by dietary curcumin, Carcinogenesis 19 (1998) 1357–1360.

[14] M. Iqbal, S.D. Sharma, Y. Okazaki, M. Fujisawa, S. Okada, Dietary supplementation of curcumin enhances antioxidant and phase II metabolizing enzymes in ddY male mice: possible role in protection against chemical carcinogenesis and toxicity, Pharmacol. Toxicol. 92 (2003) 33–38.

[15] E.A. Murphy, J.M. Davis, J.L. McClellan, B.T. Gordon, M.D. Carmichael, Curcumin's effect on intestinal inflammation and tumorigenesis in the ApcMin/+ mouse, J. Interferon Cytokine Res. 31 (2011) 219–226.

[16] J.C. Lee, P.A. Kinniry, E. Arguiri, M. Serota, S. Kanterakis, S. Chatterjee, C.C. Solomides, P. Javvadi, C. Koumenis, K.A. Cengel, M. Christofidou-Solomidou, Dietary curcumin increases antioxidant defenses in lung, ameliorates radiation-induced pulmonary fibrosis, and improves survival in mice, Radiat. Res. 173 (2010) 590–601.

[17] M.M. Sousa, I. Cardoso, R. Fernandes, A. Guimaraes, M.J. Saraiva, Deposition of transthyretin in early stages of familial amyloidotic polyneuropathy, evidence for toxicity of nonfibrillar aggregates, Am. J. Pathol. 159 (2001) 1993–2000.

[18] P.F. Teixeira, F. Cerca, S.D. Santos, M.J. Saraiva, Endoplasmic reticulum stress associated with extracellular aggregates. Evidence from transthyretin deposition in familial amyloid polyneuropathy, J. Biol. Chem. 281 (2006) 21998–22003.

[19] B. Macedo, A.R. Batista, N. Ferreira, M.R. Almeida, M.J. Saraiva, Anti-apoptotic treatment reduces transthyretin deposition in a transgenic mouse model of Familial Amyloidotic Polyneuropathy, Biochim. Biophys. Acta 1782 (2008) 517–522.

[20] K. Ono, K. Hasegawa, H. Naiki, M. Yamada, Curcumin has potent anti-amyloidogenic effects for Alzheimer's beta-amyloid fibrils in vitro, J. Neurosci. Res. 75 (2004) 742–750.

[21] F. Yang, G.P. Lim, A.N. Begum, O.J. Ubeda, M.R. Simmons, S.S. Ambegaokar, P.P. Chen, R. Kayed, C.G. Glabe, S.A. Frautschy, G.M. Cole, Curcumin inhibits formation of amyloid beta oligomers and fibrils, binds plaques, and reduces amyloid in vivo, J. Biol. Chem. 280 (2005) 5892–5901.

[22] M. Garcia-Alloza, L.A. Borrelli, A. Rozkalne, B.T. Hyman, B.J. Bacskai, Curcumin labels amyloid pathology in vivo, disrupts existing plaques, and partially restores distorted neurites in an Alzheimer mouse model, J. Neurochem. 102 (2007) 1095–1104.

[23] M.A. Hickey, C. Zhu, V. Medvedeva, R.P. Lerner, S. Patassini, N.R. Franich, P. Maiti, S.A. Frautschy, S. Zeitlin, M.S. Levine, M.F. Chesselet, Improvement of neuropathology and transcriptional deficits in CAG 140 knock-in mice supports a beneficial effect of dietary curcumin in Huntington's disease, Mol. Neurodegener. 7 (2012) 12.

[24] R. Pullakhandam, P.N. Srinivas, M.K. Nair, G.B. Reddy, Binding and stabilization of transthyretin by curcumin, Arch. Biochem. Biophys. 485 (2009) 115–119.

[25] A. Goel, A.B. Kunnumakkara, B.B. Aggarwal, Curcumin as "Curecumin": from kitchen to clinic, Biochem. Pharmacol. 75 (2008) 787–809.

[26] S. Perkins, R.D. Verschoyle, K. Hill, I. Parveen, M.D. Threadgill, R.A. Sharma, M.L. Williams, W.P. Steward, A.J. Gescher, Chemopreventive efficacy and pharmacokinetics of curcumin in the min/+ mouse, a model of familial adenomatous polyposis, Cancer Epidemiol. Biomarkers Prev. 11 (2002) 535–540.

[27] M.J. Saraiva, J. Magalhaes, N. Ferreira, M.R. Almeida, Transthyretin deposition in familial amyloidotic polyneuropathy, Curr. Med. Chem. 19 (2012) 2304–2311.

[28] J.T. Guo, J. Yu, D. Grass, F.C. de Beer, M.S. Kindy, Inflammation-dependent cerebral deposition of serum amyloid a protein in a mouse model of amyloidosis, J. Neurosci. 22 (2002) 5900–5909.

[29] B. Macedo, J. Magalhães, A.R. Batista, M.J. Saraiva, Carvedilol treatment reduces transthyretin deposition in a familial amyloidotic polyneuropathy mouse model, Pharmacol. Res. 62 (2010) 514–522.

[30] G.P. Lim, T. Chu, F. Yang, W. Beech, S.A. Frautschy, G.M. Cole, The curry spice curcumin reduces oxidative damage and amyloid pathology in an Alzheimer transgenic mouse, J. Neurosci. 21 (2001) 8370–8377.

[31] A.N. Begum, M.R. Jones, G.P. Lim, T. Morihara, P. Kim, D.D. Heath, C.L. Rock, M.A. Pruitt, F. Yang, B. Hudspeth, S. Hu, K.F. Faull, B. Teter, G.M. Cole, S.A. Frautschy, Curcumin structure-function, bioavailability, and efficacy in models of neuroinflammation and Alzheimer's disease, J. Pharmacol. Exp. Ther. 326 (2008) 196–208.

[32] M. Fiala, P.T. Liu, A. Espinosa-Jeffrey, M.J. Rosenthal, G. Bernard, J.M. Ringman, J. Sayre, L. Zhang, J. Zaghi, S. Dejbakhsh, B. Chiang, J. Hui, M. Mahanian, A. Baghaee, P. Hong, J. Cashman, Innate immunity and transcription of MGAT-III and Toll-like receptors in Alzheimer's disease patients are improved by bisdemethoxycurcumin, Proc. Natl. Acad. Sci. U. S. A. 104 (2007) 12849–12854.

[33] S. Gagliardi, S. Ghirmai, K.J. Abel, M. Lanier, S.J. Gardai, C. Lee, J.R. Cashman, Evaluation in vitro of synthetic curcumins as agents promoting monocytic gene expression related to β-amyloid clearance, Chem. Res. Toxicol. 25 (2012) 101–112.

[34] H.E. Purkey, M.I. Dorrell, J.W. Kelly, Evaluating the binding selectivity of transthyretin amyloid fibril inhibitors in blood plasma, Proc. Natl. Acad. Sci. 98 (2001) 566–5571.

[35] T. Coelho, L.F. Maia, A. Martins da Silva, M. Waddington Cruz, V. Planté-Bordeneuve, P. Lozeron, O.B. Suhr, J.M. Campistol, I.M. Conceição, H.H. Schmidt, P. Trigo, J.W. Kelly, R. Labaudinière, J. Chan, J. Packman, A. Wilson, D.R. Grogan, Tafamidis for transthyretin familial amyloid polyneuropathy: a randomized, controlled trial, Neurology 79 (2012) 785–792.

[36] N. Ferreira, I. Cardoso, M.R. Domingues, R. Vitorino, M. Bastos, G. Bai, M.J. Saraiva, M.R. Almeida, Binding of epigallocatechin-3-gallate to transthyretin modulates its amyloidogenicity, FEBS Lett. 583 (2009) 3569–3576.

[37] N. Ferreira, M.J. Saraiva, M.R. Almeida, Epigallocatechin-3-gallate as a potential therapeutic drug for TTR-related amyloidosis: "in vivo" evidence from FAP mice models, PLoS One 7 (2012) e29933.

[38] M. Miyata, T. Sato, M. Kugimiya, M. Sho, T. Nakamura, S. Ikemizu, M. Chirifu, M. Mizuguchi, Y. Nabeshima, Y. Suwa, H. Morioka, T. Arimori, M.A. Suico, T. Shuto, Y. Sako, M. Momohara, T. Koga, S. Morino-Koga, Y. Yamagata, H. Kai, The crystal structure of the green tea polyphenol (−)-epigallocatechin gallate-transthyretin complex reveals a novel binding site distinct from the thyroxine binding site, Biochemistry 49 (2010) 6104–6114.

[39] A.V. Kristen, S. Lehrke, S. Buss, D. Mereles, H. Steen, P. Ehlermann, S. Hardt, E. Giannitsis, R. Schreiner, U. Haberkorn, P.A. Schnabel, R.P. Linke, C. Röcken, E.E. Wanker, T.J. Dengler, K. Altland, H.A. Katus, Green tea halts progression of cardiac transthyretin amyloidosis: an observational report, Clin. Res. Cardiol. 101 (2012) 805–813.

[40] E. Burgos-Morón, J.M. Calderón-Montaño, J. Salvador, A. Robles, M. López-Lázaro, The dark side of curcumin, Int. J. Cancer 126 (2010) 1771–1775.

[41] P. Anand, A.B. Kunnumakkara, R.A. Newman, B.B. Aggarwal, Bioavailability of curcumin: problems and promises, Mol. Pharm. 4 (2007) 807–818.